Title

Validation of a prognostic multi-gene signature in high-risk neuroblastoma using the high throughput digital NanoString nCounter™ system

Journal

Molecular Oncology, 8(3)

ISSN

1574-7891

Authors

Stricker, Thomas P
La Madrid, Andres Morales
Chlenski, Alexandre
et al.

Publication Date

2014-05-01

DOI

10.1016/j.molonc.2014.01.010

Peer reviewed

MOLECULAR ONCOLOGY 8 (2014) 669–678

available at www.sciencedirect.com

ScienceDirect

www.elsevier.com/locate/molonc

Validation of a prognostic multi-gene signature in high-risk neuroblastoma using the high throughput digital NanoString nCounter™ system

Thomas P. Stricker[a,1], Andres Morales La Madrid[b,1,2], Alexandre Chlenski[b], Lisa Guerrero[b], Helen R. Salwen[b], Yasmin Gosiengfiao[c], Elizabeth J. Perlman[d], Wayne Furman[e], Armita Bahrami[f], Jason M. Shohet[g], Peter E. Zage[g], M. John Hicks[h], Hiroyuki Shimada[i], Rie Suganuma[i], Julie R. Park[j,k], Sara So[j,k], Wendy B. London[l,m], Peter Pytel[n], Kirsteen H. Maclean[o], Susan L. Cohn[b,*]

[a]Department of Pathology, Microbiology and Immunology, Vanderbilt University, Nashville, TN, USA
[b]Department of Pediatrics, Comer Children's Hospital, University of Chicago, Chicago, IL, USA
[c]Department of Pediatrics, Ann and Robert H. Lurie Children's Hospital of Chicago, Northwestern University Feinberg School of Medicine, Chicago, IL, USA
[d]Department of Pathology, Ann and Robert H. Lurie Children's Hospital of Chicago, Northwestern University Feinberg School of Medicine, Chicago, IL, USA
[e]Department of Hematology/Oncology, St. Jude Children's Research Hospital, Memphis, TN, USA
[f]Department of Pathology, St. Jude Children's Research Hospital, Memphis, TN, USA
[g]Department of Pediatrics, Texas Children's Cancer Center, Baylor College of Medicine, Houston, TX, USA
[h]Department of Pathology, Texas Children's Cancer Center, Baylor College of Medicine, Houston, TX, USA
[i]Department of Pathology and Laboratory Medicine, Children's Hospital Los Angeles, Los Angeles, CA, USA
[j]Department of Pediatrics, Seattle Children's Hospital, University of Washington, Seattle, WA, USA
[k]Fred Hutchinson Cancer Research Center, Seattle, WA, USA
[l]Children's Oncology Group Statistics and Data Center, Boston, MA, USA
[m]Boston Children's Hospital/Dana-Farber Cancer Institute, Boston, MA, USA
[n]Department of Pathology, Comer Children's Hospital, University of Chicago, Chicago, IL, USA
[o]NanoString Technologies, Seattle, WA, USA

ARTICLE INFO

Article history:
Received 11 November 2013
Received in revised form
24 December 2013

ABSTRACT

Microarray-based molecular signatures have not been widely integrated into neuroblastoma diagnostic classification systems due to the complexities of the assay and requirement for high-quality RNA. New digital technologies that accurately quantify gene expression using RNA isolated from formalin-fixed paraffin embedded (FFPE) tissues are now available. In this study, we describe the first use of a high-throughput digital system

Abbreviations: FFPE, formalin-fixed paraffin embedded; INRG, International Neuroblastoma, Risk Group; COG, Children's Oncology Group; H&E, hematoxylin and eosin; SD, standard deviations; EFS, event-free survival; OS, overall survival; SE, standard error; PCA, Principal Components Analysis.

* *Corresponding author.* Department of Pediatrics, Comer Children's Hospital, University of Chicago, KCBD, Rm 5100, 900 E. 57th Street, Chicago, IL 60637, USA. Tel.: +1 773 702 2571; fax: +1 773 834 1329.
E-mail address: scohn@peds.bsd.uchicago.edu (S.L. Cohn).
[1] Authors contributed equally to this study.
[2] Present address: Department of Pediatric Oncology, Hospital Sant Joan de Déu, Barcelona, Spain.

http://dx.doi.org/10.1016/j.molonc.2014.01.010

Accepted 21 January 2014
Available online 31 January 2014

Keywords:
High-risk neuroblastoma
Gene signature
Molecular classifier
NanoString
nCounter

to assay the expression of genes in an "ultra-high risk" microarray classifier in FFPE high-risk neuroblastoma tumors. Customized probes corresponding to the 42 genes in a published multi-gene neuroblastoma signature were hybridized to RNA isolated from 107 FFPE high-risk neuroblastoma samples using the NanoString nCounter™ Analysis System. For classification of each patient, the Pearson's correlation coefficient was calculated between the standardized nCounter™ data and the molecular signature from the microarray data. We demonstrate that the nCounter™ 42-gene panel sub-stratified the high-risk cohort into two subsets with statistically significantly different overall survival ($p = 0.0027$) and event-free survival ($p = 0.028$). In contrast, none of the established prognostic risk markers (age, stage, tumor histology, *MYCN* status, and ploidy) were significantly associated with survival. We conclude that the nCounter™ System can reproducibly quantify expression levels of signature genes in FFPE tumor samples. Validation of this microarray signature in our high-risk patient cohort using a completely different technology emphasizes the prognostic relevance of this classifier. Prospective studies testing the prognostic value of molecular signatures in high-risk neuroblastoma patients using FFPE tumor samples and the nCounter™ System are warranted.

1. Introduction

Neuroblastoma, the most frequent extracranial solid tumor of childhood, exhibits a broad range of clinical behavior and varying response to treatment (Maris et al., 2007). To ensure that therapy is appropriately tailored, efforts to identify variables that accurately predict outcome have been ongoing for more than 35 years. Recently, an International Neuroblastoma Risk Group (INRG)[4] Classification System has been established that utilizes 7 prognostic variables to stratify patients into very low-, low-, intermediate-, or high-risk cohorts (Cohn et al., 2009). Although outcome is excellent for non-high-risk patients, almost half of all patients are classified as high-risk, and less than 50% will be cured with current treatment strategies. At the time of diagnosis, it is currently not possible to distinguish the subset of high-risk patients who will achieve long-term survival from those who will develop progressive disease.

The prognostic value of gene expression profiles has been recently evaluated using microarray technologies, and numerous low- and high-risk neuroblastoma signatures have been discovered, tested, and validated (Abel et al., 2011; De Preter et al., 2010; Garcia et al., 2012; Schramm et al., 2005; Schulte et al., 2010; Vermeulen et al., 2009; Wei et al., 2004). Some of these signatures can sub-stratify patients with high-risk neuroblastoma, identifying a subset of high-risk patients with significantly worse survival, or an "ultra-high-risk" group (Abel et al., 2011; Asgharzadeh et al., 2006; De Preter et al., 2010; Garcia et al., 2012). However, incorporating molecular signatures into diagnostic classification systems has proven to be difficult because microarray analysis requires frozen tumor tissue to yield high quality RNA, and these samples are rarely available. The microarray-based assays are also expensive and require complex statistical analyses. The nCounter™ System overcomes these limitations. This system utilizes simple technology that captures and counts individual mRNA transcripts with high levels of sensitivity, linearity, multiplex capability, and digital readout. Importantly, different sample types, including highly degraded RNA from FFPE material, can be utilized (Fernandez et al., 2012; Kulkarni, 2011; Payton et al., 2009; Stricker et al., 2013), and recent studies using the nCounter™ System have validated expression signatures obtained using microarray technology (Kulkarni, 2011; Malkov et al., 2009; Northcott et al., 2012).

Here we describe the first use of a high-throughput digital system to assay the expression of a published "ultra-high risk" neuroblastoma molecular classifier (De Preter et al., 2010). The 42-gene signature was built from a meta-analysis of neuroblastoma studies performed using oligonucleotide microarray platforms. We show that the prognostic value of this microarray-derived gene signature was validated in a cohort of 107 high-risk neuroblastoma patients using nCounter™ technology and RNA isolated from FFPE high-risk neuroblastoma tumor samples.

2. Materials and methods

2.1. *Tumor samples*

Neuroblastoma patients from Comer Children's Hospital, St. Jude Children's Research Hospital, Ann & Robert H. Lurie Children's Hospital of Chicago, Texas Children's Hospital, Seattle Children's Hospital, and Children's Hospital Los Angeles were diagnosed from 1993 to 2011 and classified as high-risk based on Children's Oncology Group (COG) criteria (Maris, 2010). Medical records were abstracted at each institution and clinical data including age at diagnosis, stage, *MYCN* status, ploidy, histology, and outcome were collected. The patients were staged according to the International Neuroblastoma Staging System (Brodeur et al., 1993) and tumor histology was defined as favorable or unfavorable using the International Neuroblastoma Pathologic Classification (INPC) System (Shimada et al., 1999). A hematoxylin and eosin (H&E) stained section and two to four FFPE scrolls of diagnostic tumor tissue were sent to the University of Chicago. The stained tissue sections were reviewed by a pathologist (PP), and the percentage of viable and necrotic tumor, lymphoid infiltrates and other tissue elements including connective tissue and stroma were assessed.

Table 1 – Sequence-specific probes constructed for the analysis of 107 high-risk neuroblastoma tumors using the nCounter™ System.

De Preter et al.	Refseq ID	Targeted region	Reference genes	Refseq ID	Targeted region
AHCY	NM_000687.2	1805–1905	ACSM3	NM_005622.3	955–1055
AKR1C1	NM_001353.5	1210–1310	BRD4	NM_014299.2	745–845
ARHGEF7	NM_001113511.1	1275–1375	CLTC	NM_004859.2	290–390
BIRC5	NM_001012270.1	1095–1195	CRYBB3	NM_004076.3	230–330
CADM1	NM_001098517.1	1071–1171	DHX57	NM_198963.1	3888–3988
CAMTA2	NM_015099.2	1573–1673	EIF5A2	NM_020390.5	450–550
CDCA5	NM_080668.3	320–420	GAPDH	NM_002046.3	35–135
CDKN3	NM_001130851.1	390–490	GNAI2	NM_002070.2	1000–1100
CLSTN1	NM_001009566.1	935–1035	GUSB	NM_000181.1	1350–1450
DDC	NM_000790.3	1195–1295	HDAC3	NM_003883.2	1455–1555
DPYSL3	NM_001387.2	4790–4890	HPRT1	NM_000194.1	240–340
ECEL1	NM_004826.2	2443–2543	N4BP1	NM_153029.3	2495–2595
EPB41L3	NM_012307.2	2455–2555	OAZ1	NM_004152.2	313–413
EPHA5	NM_004439.4	2855–2955	PGK1	NM_000291.2	1030–1130
EPN2	NM_014964.4	285–385	PTK6	NM_005975.2	1715–1815
FYN	NM_002037.3	765–865	RPL23A	NM_000984.5	611–711
GNB1	NM_002074.2	2165–2265	RPS6KB2	NM_003952.2	980–1080
HIVEP2	NM_006734.3	5715–5815	SDHA	NM_004168.1	230–330
INPP1	NM_001128928.1	1515–1615	SUFU	NM_016169.2	4380–4480
MAP7	NM_003980.3	1085–1185	TRAPPC3	NM_014408.3	212–312
MAPT	NM_001123066.2	5605–5705	TUBB	NM_178014.2	320–420
MCM2	NM_004526.2	2945–3045	UBC	NM_021009.3	1875–1975
MRPL3	NM_007208.2	350–450			
MYCN	NM_005378.4	1545–1645			
NCAN	NM_004386.2	4330–4430			
NME1	NM_000269.2	500–600			
NRCAM	NM_001037132.1	4955–5055			
NTRK1	NM_001012331.1	1365–1465			
ODC1	NM_002539.1	950–1050			
PAICS	NM_001079524.1	2604–2704			
PLAGL1	NM_001080951.1	64–164			
PMP22	NM_000304.2	1644–1744			
PRKACB	NM_002731.2	835–935			
PRKCZ	NM_002744.4	771–871			
PTN	NM_002825.5	80–180			
PTPRN2	NM_002847.3	2865–2965			
SCG2	NM_003469.3	1400–1500			
SLC24A5	NM_205850.2	410–510			
SNAPC1	NM_003082.3	143–243			
TYMS	NM_001071.1	555–655			
ULK2	NM_014683.2	2340–2440			
WSB1	NM_015626.8	1410–1510			

Only cases with >50% viable neuroblastoma tumor cells were selected for expression profiling. This study was approved by the Institutional Review Board at the University of Chicago and at each of the collaborating institutions.

2.2. RNA isolation

RNA was isolated using the RNeasy® FFPE kit (Qiagen, Valencia, CA) from two 10-μm sections from each sample. RNA concentration was quantified using UV spectroscopy (Nanodrop Technologies, Wilmington, DE) and integrity assessed using a Bioanalyzer 2100 and RNA Nano Chip assay (Agilent Technologies, Wilmington, DE).

2.3. Codeset design and expression quantification

Details of the nCounter™ technology (NanoString Technologies, Seattle, WA) have been reported previously (Geiss et al., 2008; Kulkarni, 2011). Briefly, NanoString designed and manufactured customized probes corresponding to the 42 genes in a previously reported prognostic signature (De Preter et al., 2010) (Table 1). A codeset specific to a 100-base region of the target mRNA was designed using a 3′ biotinylated capture probe and a 5′ reporter probe tagged with a specific fluorescent barcode; creating two sequence-specific probes for each target transcript. Probes were hybridized to 100 ng of total RNA for 19 h at 65 °C and applied to the nCounter™ Preparation Station for automated removal of excess probe and immobilization of probe-transcript complexes on a streptavidin-coated cartridge. Data were collected using the nCounter™ Digital Analyzer by counting the individual barcodes.

2.4. Data processing and class prediction analysis

Each codeset included probes for the 42-gene signature, spiked-in External RNA Control Consortium positive and

Table 2 – Clinical and biological characteristics of patient cohort.

Characteristic	No	%	5 year EFS +/– SE	P value	5-year OS +/– SE	P value
Age						
≤18 months	24	22.4	35.7 +/– 10.1	0.0761	48.6 +/– 10.5	0.3985
>18 months	83	77.6	44.9 +/– 6.0		52.8 +/– 6.1	
INSS stage						
2,3	20	18.7	50.5 +/– 12	0.5448	49.8 +/– 12.0	0.7994
4	87	81.3	40.8 +/– 5.7		52.4 +/– 5.9	
Histology[a]						
Favorable	10	9.3	33.3 +/– 17.2	0.3083	45.0 +/– 17.4	0.4633
Unfavorable	72	67.3	40.8 +/– 6.4		49.4 +/– 6.5	
Unknown	25	23.4	49.6 +/– 10.3		61 +/– 0.1	
MYCN Status						
Unamplified	38	35.5	46.5 +/– 8.7	0.2901	54.0 +/– 8.8	0.6345
Amplified	61	57.0	42.6 +/– 6.8		53.0 +/– 6.9	
Unknown	8	7.5	30.0 +/– 17.5		36 +/– 0.2	
Ploidy						
Hyperdiploid	45	42.1	44.4 +/– 7.9	0.3956	52.4 +/– 8.1	0.0923
Diploid	36	33.6	33.1 +/– 8.9		42.6 +/– 9.1	
Unknown	26	24.3	51.7 +/– 10.6		63.6 +/– 10.3	

[a] International Neuroblastoma Pathologic Classification (Shimada et al., 1999).

negative controls, and reference housekeeping genes (Table 1). Housekeeping genes were selected by analyzing published neuroblastoma microarray datasets (Asgharzadeh et al., 2006; Oberthuer et al., 2010; Wang et al., 2006), binning genes into low- medium- and highly-expressed, and then selecting 3 genes for each category with minimal variance across samples.

Background hybridization was determined using spiked-in negative controls. All signals below mean background plus 2 standard deviations (SD) were considered to be below the limits of detection, and set to mean background. A normalization factor was calculated from the spiked in exogenous positive controls in each sample and applied to the raw counts from the nCounter™ output data. Then, a content normalization factor was calculated from the Geomean of the reference genes and applied to the data previously normalized by the positive control. Probesets were produced in two batches, and several samples were run with both sets of probes to generate a per gene batch correction factor that was applied across the entire data set. Each sample was run in duplicate, and for most analyses, the mean of the sample pairs was used.

2.5. *Statistical analysis*

The methods of Kaplan–Meier (Kaplan and Meier, 1958) were used to generate event-free survival (EFS) and overall survival (OS) curves for the entire cohort and for subgroups stratified by established risk factors using Prism 5 (GraphPad Software, Inc., La Jolla, CA). The curves were compared using a log-rank test. Five-year EFS and OS rates were expressed as the estimate ± the standard error (SE).

To test the prognostic signature described by De Preter and colleagues, cross-platform data for the 42 genes from the 250 patients in their training set were obtained (De Preter et al., 2010). Following methods reported by these investigators (De Preter et al., 2010), a prognostic vector was created by subtracting the mean expression value in patients with EFS of at least 1000 days from the mean expression value from the patients who died of disease for each of the 42 genes. For classification of each of the 107 individuals in our study, the Spearman's correlation coefficient was calculated between the log transformed, normalized nCounter™ data, and the vector from the De Preter training data. Patients with a negative correlation coefficient were predicted to have low-molecular risk and a favorable prognosis, whereas patients with a positive correlation had high-molecular risk and an unfavorable prognosis. Survival functions (low versus high-molecular risk) were compared with the log-rank test using the survival package in R. Heatmaps were generated using Heatmap.2, and Principal Components Analysis (PCA) was performed using the pcaMethods packages in R. MYCN targets were identified by taking the union of the following gene sets in MdbSig3.0: MYC_amplified_leukemia, MYC_amplified, MYC_targets_up, and MYC_targets_down.

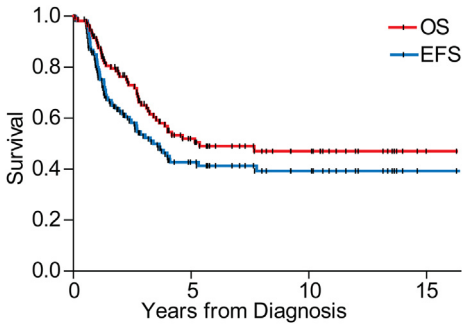

Figure 1 – Kaplan–Meier curves of OS and EFS of the entire cohort of patients with high-risk neuroblastoma ($n = 107$).

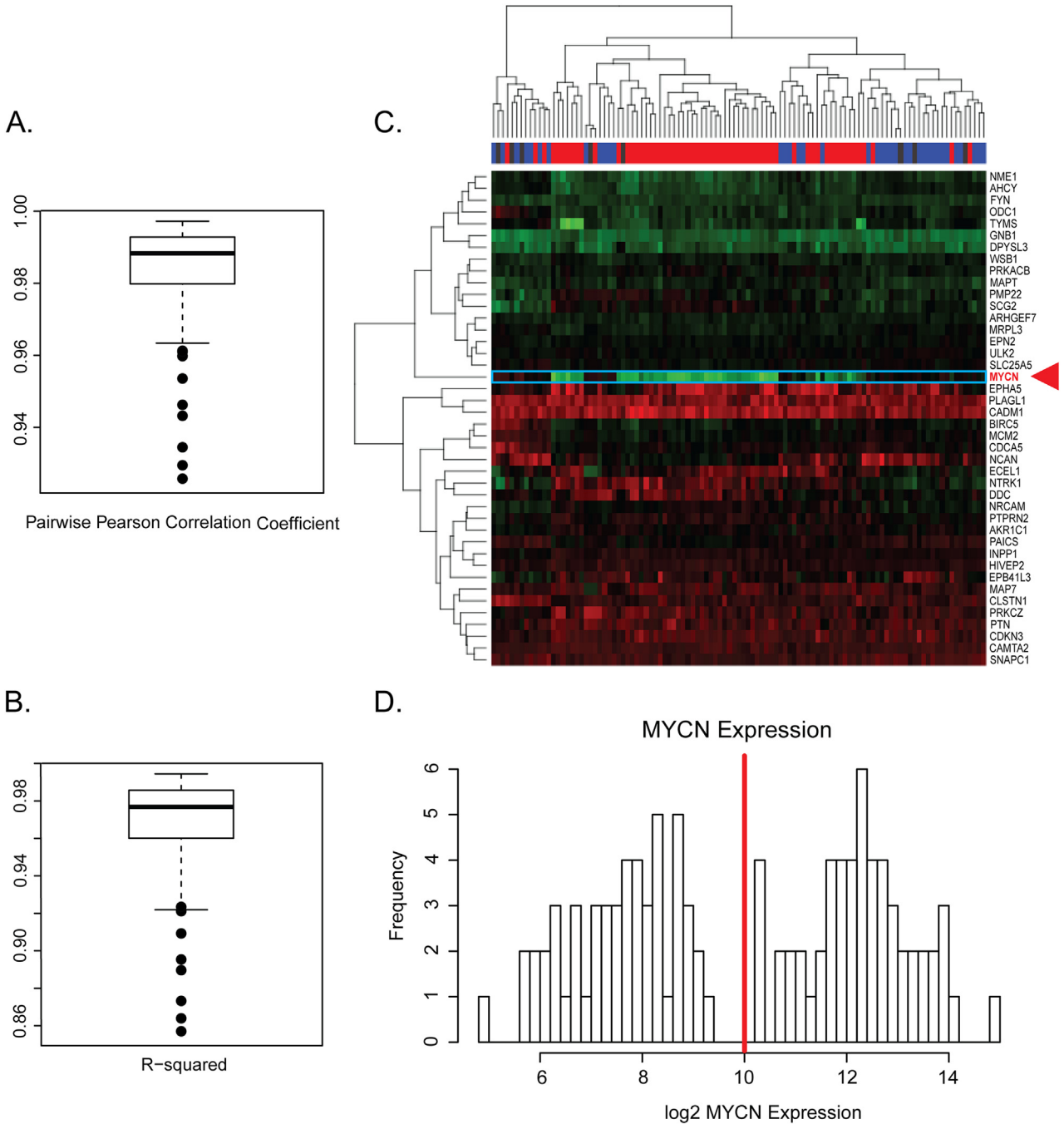

Figure 2 – A) Boxplots of Pearson Correlation Coefficients for all sample duplicates show that all pairs are highly correlated. B) Boxplot of the R-squared for all duplicates derived from a linear regression shows that all duplicates are highly correlated. C) Unsupervised hierarchical clustering of the mean of duplicates for all 107 samples by expression levels of 42 genes as measured by the nCounter™ System. The bar at the top denotes *MYCN* amplification status, with red = amplified, blue = non-amplified, and gray = unknown. D) Histogram plotting the *MYCN* expression levels for each sample. Samples clearly segregate into low *MYCN* and high *MYCN* expression.

3. Results

3.1. *Analytic cohort of 107 high-risk neuroblastoma patients*

A total of 138 high-risk patients with available paraffin-embedded material were identified at the 6 participating institutions. Review of the medical records revealed that 5 cases were misclassified as high-risk. Tumor tissue was not available in 5 cases, as the diagnosis was made using bone marrow samples. In 10 cases, tumor cellularity was <50%. RNA was isolated from 118 tumors. For 11 samples the data quality was poor as determined by correction factors >10, >20% of the genes were expressed below the threshold, and/or overall means were 3 or more SD above or below the mean for all samples following correction and normalization. Although

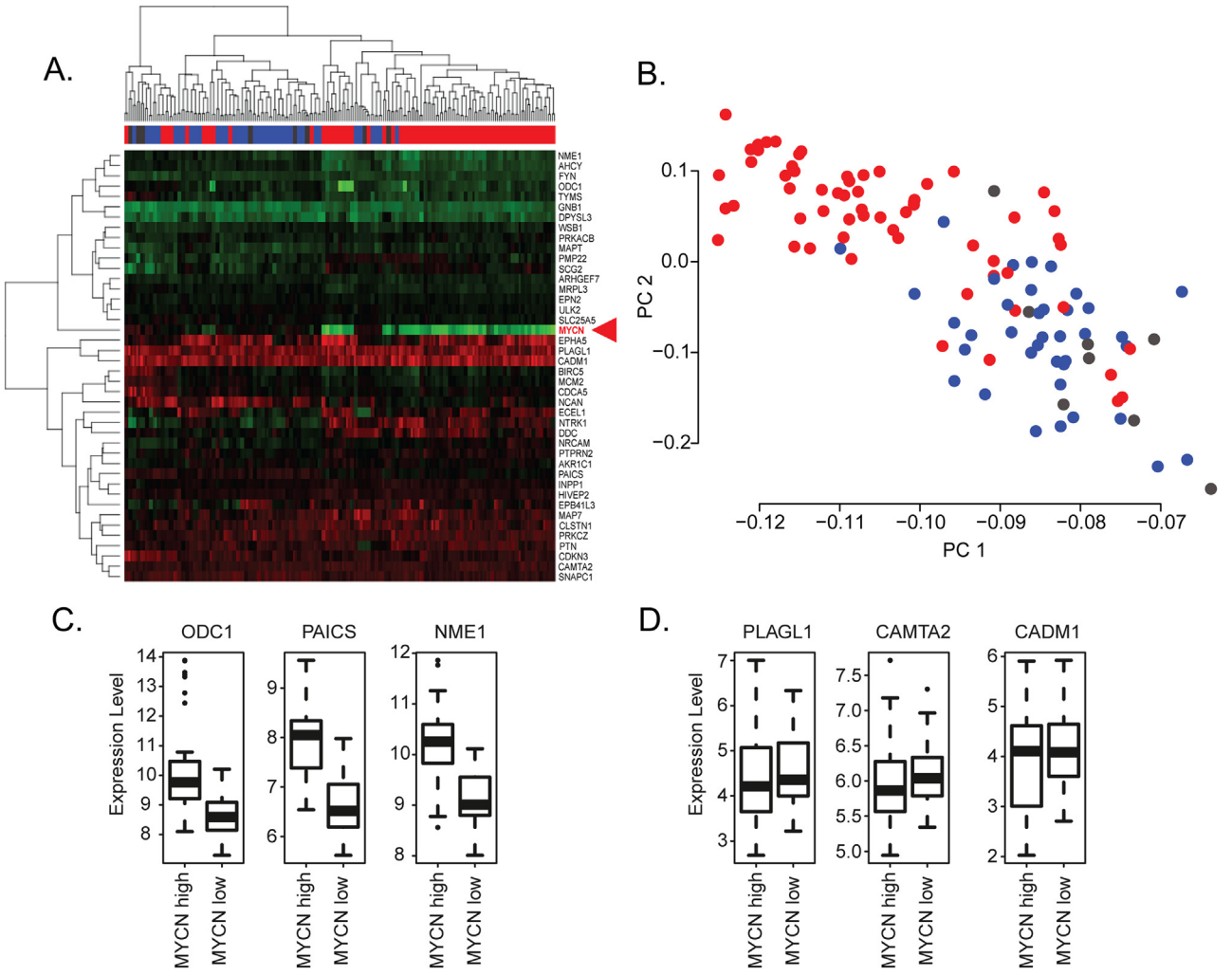

Figure 3 – Unsupervised clustering of 42-genes shows a strong association with *MYCN* amplification status. A) Unsupervised hierarchical clustering of all independent samples by expression levels of the 42-genes in the high-risk signature. The bar at the top denotes *MYCN* amplification status, with red = amplified, blue = non-amplified, and gray = unknown. B) First 2 principal components in a principal components analysis, based on the mean level of expression of 42 genes in 107 samples. Color denotes *MYCN* amplification status as above. C) Boxplots of gene expression levels for known MYC targets ODC1, PAICS, and NME1 show that they are strongly differentially expressed between *MYCN* amplified versus non-amplified cases. D) Boxplots of gene expression levels for genes in the 42-gene signature that are not associated with MYCN expression or *MYCN* status.

many of samples with poor data quality were needle-core biopsies, we were able to generate high quality expression data from 8 core needle biopsy samples. Thus, the size of the core needle biopsies and the amount of viable tumor in these samples are important determinants of data quality. We were able to generate high quality expression data for 107/118 cases (90.7%), using FFPE material, and these patients comprised the analytic cohort for this study.

Patients ranged in age from 3 days to 184 months, with a mean of 38 months. Eighty-three (77.6%) patients were older than 18 months (Table 2). Eighty-seven (81.3%) patients had stage 4 disease, and *MYCN* amplification was detected in tumors from 61 patients (57%). All patients were either enrolled on or treated according to a cooperative group clinical trial or institutional high-risk neuroblastoma protocols (Furman et al., 2012; Kletzel et al., 2002; Kreissman et al., 2013; Matthay et al., 2009; Santana et al., 2005; Wagner et al., 2004). Five-year EFS and OS rates ±SE for the entire cohort were 43% ± 5.2% and 52% ± 5.3%, respectively (Figure 1). Age at diagnosis, stage of disease, tumor histology, *MYCN* status, and ploidy were not statistically significantly predictive of outcome (Table 2).

3.2. *Integrity of RNA from FFPE blocks is sufficient for nCounter™ analysis*

The integrity of the RNA determined by the Bioanalyzer varied from a RIN of 1.2–2.8, confirming that the RNA purified from FFPE blocks is highly degraded. Although RNA with RINs of 7.5 or greater is generally recommended for microarray experiments, chains that are at least 100 base pairs long were suitable for hybridization with the capture and reporter probes using the nCounter™ system.

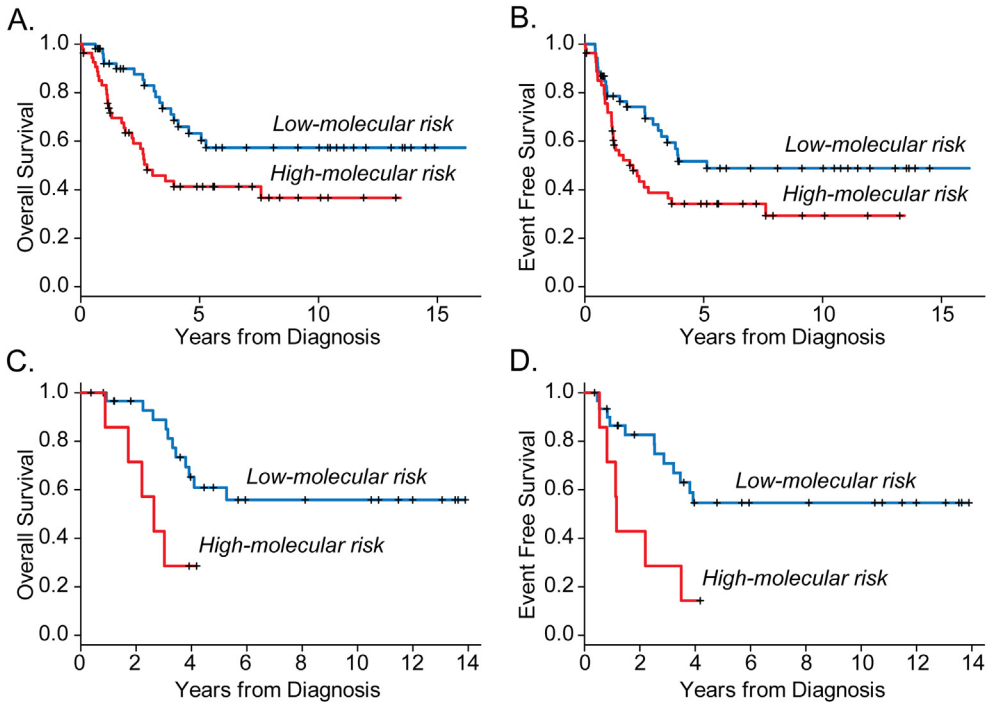

Figure 4 – Kaplan–Meier curves of OS (A) and EFS (B) for 107 high-risk neuroblastoma patients classified using the 42-gene prognostic signature analyzed using the nCounter™ System. OS and EFS were statistically significantly worse for patients with high-molecular risk neuroblastomas compared to those with low-molecular risk tumors ($p = 0.0027$ and $p = 0.028$, respectively). Kaplan–Meier curves of OS (C) and EFS (D) for non-*MYCN* amplified cases. OS and EFS were statistically significantly worse for patients with high-molecular risk neuroblastomas compared to those with low-molecular risk tumors ($p = 0.0056$ and $p = 0.011$, respectively).

3.3. *Gene expression cluster analysis shows correlation with* MYCN *status*

The nCounter™ measurements were highly reproducible. Pearson correlation coefficients were calculated for each of the duplicate samples and ranged between 0.925 and 0.997 (mean of 0.98) (Figure 2A). Furthermore, a linear regression was performed on all pairs, and the R-squared values ranged between 0.855 and 0.995 with a mean of 0.96 (Figure 2B). Unsupervised clustering of the 42 genes tested within our cohort showed that samples clustered into three groups, largely defined by expression of *MYCN* (Figure 3A). The *MYCN* high expressing group consisted of cases with *MYCN* amplified tumors, but there were some non-amplified cases in this group as well. Interestingly, although these tumors clustered with the *MYCN* amplified tumors, their *MYCN* expression levels were lower than that observed in the amplified tumors, indicating that they are similar to amplified tumors on the basis of other genes in the signature. The other two groups had lower levels of expression of *MYCN*. Of note, while these were mostly non-amplified tumors, there were some amplified tumors in these clusters that, while they expressed *MYCN*, they did so at levels closer to non-amplified tumors. The heat map demonstrates that duplicate samples were highly correlated; for every sample, the most closely related sample was the replicate (Figure 3A). Thus, the mean expression level for each replicate was calculated and used in all subsequent experiments.

A heat map of the mean values showed similar segregation of tumors by *MYCN* expression (Figure 2C). PCA of the expression levels for 42 genes also demonstrated a strong separation between samples with versus without *MYCN* amplification (Figure 3B). *MYCN* gene expression clearly segregated into high and low expression groups, and the level of expression correlated strongly with *MYCN* amplification status (Figure 2D). Eighty-nine percent (54/61) of *MYCN* amplified cases also had high expression of *MYCN*. Likewise, of the samples with high *MYCN* expression, only 4 did not have *MYCN* amplification. In addition, high *MYCN* gene expression correlated with expression of known MYC target genes (*i.e. ODC1, PAICS, NME1*) (Ben-Yosef et al., 1998) (Figure 3C). De Preter and colleagues noted that 12 of the 42 genes in the signature are known targets of MYCN (De Preter et al., 2010). We found that expression of all 12 of these genes strongly correlated with *MYCN* status in our cohort. To specifically determine the correlation between each of the genes in the signature and *MYCN* status, differentially expressed genes in the *MYCN* amplified versus non-amplified cases were quantified via linear model, followed by correction for multiple hypothesis testing using Storey's *q*-value method (Storey, 2002). Twenty-eight of the 42 genes in the signature were statistically significantly differentially expressed in the *MYCN* amplified cases compared to the non-amplified tumors, including the known MYC targets *CAMTA1*, *NME1*, and *NTRK1*. However, 14 additional genes, including *PLAGL1, AKR1C1, ARHGEF7, CADM1, CAMTA2, EPB41L3*, and *FYN*, showed little correlation with *MYCN* status (Figure 3C and D).

3.4. *The multi-gene expression signature analyzed with the nCounter™ system sub-stratifies high-risk neuroblastoma*

The nCounter™ 42-gene panel sub-stratified the cohort of 107 high-risk patients into two groups with statistically significantly different outcome, replicating the results of De Preter et al. (2010) Patients with low- versus high-molecular risk tumors had OS rates of 57.3% ± 7.8% versus 36.7% ± 7.7%, respectively ($p = 0.0027$) (Figure 4A), and EFS of 48.8% ± 7.7% versus 29.3% ± 7.4% ($p = 0.028$) (Figure 4B). The 42-gene signature was also prognostic within the subset of 38 high-risk patients with non-*MYCN* amplified tumors, with OS of 55.8% ± 10% versus 28.6% ± 17% ($p = 0.0056$) for patients with low vs high-risk molecular tumors (Figure 4C), and EFS of 54.6% ± 9.8% versus 14.3% ± 13.2%, respectively ($p = 0.011$) (Figure 4D).

4. Discussion

In this study, we validated the prognostic significance of a published neuroblastoma microarray signature that was previously shown to sub-stratify high-risk patients into cohorts with significantly different survival (De Preter et al., 2010) using high throughput digital technology and RNA isolated from 107 FFPE high-risk tumors. The cohort of high-risk patients with worse outcome is considered at "ultra-high risk" for relapse. The nCounter™ system requires very small amounts of RNA, and reliable results can be obtained even if the RNA is highly degraded. This technology has numerous advantages over microarray methodology including the ability to analyze gene expression using FFPE tumor tissue as starting material. The workflow does not involve enzymatic and amplification steps, thus reducing the risk of additional technical errors and the introduction of bias in the results. Furthermore, this digital technology is less time consuming, requires only a simple data analysis and normalization strategy, and is less expensive and more reproducible (Malkov et al., 2009).

The multi-gene signature analyzed in our study originated from an analysis of 933 neuroblastoma patients from eight independent studies (De Preter et al., 2010). This molecular classifier was established based on re-analysis of published studies with updated clinical information, re-annotation of the probe sequences, common risk definitions for training cases, and a single method for gene selection (prediction analysis of microarray) and classification (correlation analysis). Using new digital technology, we replicated the findings of De Preter et al. (2010) and show that the 42-gene classifier sub-stratified high-risk neuroblastoma patients into subsets with significantly different outcome. The signature was also prognostic within the subset of patients with tumors that lacked *MYCN* amplification. In contrast, none of the other established prognostic markers was associated with outcome.

Interestingly, although 28 of the 42 genes were statistically differentially expressed between *MYCN* amplified and non-amplified cases, the signature determined prognosis in the whole cohort as well as the non-*MYCN* amplified group. In fact, this signature was prognostic while *MYCN* status was not in our cohort. It is important to note that not all genes are associated with *MYCN* status, and thus this signature doesn't just represent *MYCN* copy number status. Indeed, it can be seen from the heatmap that while amplified and non-amplified tumors mostly cluster separately, there are non-amplified tumors clustering with the amplified tumors and vice versa. Future studies will explore the hypothesis that the expression signature, rather than *MYCN* amplification status, is a more accurate measurement of *MYCN* pathway activation, and thus, a better discriminator for outcome.

Despite the prognostic value of this 42-gene ultra-high risk signature (De Preter et al., 2010), it has not been prospectively studied or integrated into a neuroblastoma classification system, due in part to the requirement for frozen tumor and high quality RNA isolation for the microarray assay. Although frozen tumors are not readily available, the vast majority of patients with high-risk neuroblastoma have FFPE tumor samples. RNA extracted from FFPE material is typically highly degraded, and therefore of limited use in other molecular studies. The nCounter™ technology overcomes this obstacle by using relatively short 50mer probes that will hybridize efficiently with RNA chains as short as 100 base pairs (each target gene hybridizes with one capture and one reporter probe). As we show, the highly degraded RNA from FFPE tumor samples is sufficient to obtain strong gene expression signals that are highly reproducible.

The ability to identify patients who will not adequately respond to standard high-risk treatment strategies in the diagnostic setting is critical for informed treatment decisions. Prospective clinical trials will be needed to identify the most powerful prognostic classifiers for high-risk neuroblastoma patients. Using the nCounter™ System, data can be generated in ~24 h and analytic results can be obtained within a few weeks. Thus, this technology is well suited for evaluating expression signatures in newly diagnosed patients. With more precise prognostication, "ultra-high-risk" patients could be spared unnecessary acute and long-term toxicities associated with current, intensive multi-modality therapy approaches. Transitioning patients who are not likely to survive with standard therapy to alternative treatments and/or early phase clinical studies may provide the clinical benefit of more targeted, less toxic treatments and improved quality of life.

Conflict of interest

Kirsteen H. Maclean is a NanoString Technologies employee.

Acknowledgements

This work was supported by Conquer Cancer Foundation (AML); St. Baldrick's Foundation (AML); Children's Neuroblastoma Cancer Foundation (SLC); Neuroblastoma Children's Cancer Society (SLC); Elise Anderson Foundation (SLC), and The National Cancer Institute 1K08CA148912 (TPS).

REFERENCES

Abel, F., Dalevi, D., Nethander, M., Jornsten, R., De Preter, K., Vermeulen, J., Stallings, R., Kogner, P., Maris, J., Nilsson, S., 2011. A 6-gene signature identifies four molecular subgroups of neuroblastoma. Cancer Cell Int. 11, 9.

Asgharzadeh, S., Pique-Regi, R., Sposto, R., Wang, H., Yang, Y., Shimada, H., Matthay, K., Buckley, J., Ortega, A., Seeger, R.C., 2006. Prognostic significance of gene expression profiles of metastatic neuroblastomas lacking MYCN gene amplification. J. Natl. Cancer Inst. 98, 1193–1203.

Ben-Yosef, T., Yanuka, O., Halle, D., Benvenisty, N., 1998. Involvement of Myc targets in c-myc and N-myc induced human tumors. Oncogene 17, 165–171.

Brodeur, G.M., Pritchard, J., Berthold, F., Carlsen, N.L., Castle, V., Castelberry, R.P., De Bernardi, B., Evans, A.E., Favrot, M., Hedborg, F., Kaneko, M., Kemshead, J., Lampert, F., Lee, R.E.J., Look, A.T., Pearson, A.D.J., Philip, T., Roald, B., Sawada, T., Seeger, R.C., Tsuchida, Y., Voute, P.A., 1993. Revisions of the international criteria for neuroblastoma diagnosis, staging, and response to treatment. J. Clin. Oncol. 11, 1466–1477.

Cohn, S.L., Pearson, A.D., London, W.B., Monclair, T., Ambros, P.F., Brodeur, G.M., Faldum, A., Hero, B., Iehara, T., Machin, D., Mosseri, V., Simon, T., Garaventa, A., Castel, V., Matthay, K.K., Force, I.T., 2009. The international neuroblastoma risk group (INRG) classification system: an INRG task force report. J. Clin. Oncol. 27, 289–297.

De Preter, K., Vermeulen, J., Brors, B., Delattre, O., Eggert, A., Fischer, M., Janoueix-Lerosey, I., Lavarino, C., Maris, J.M., Mora, J., Nakagawara, A., Oberthuer, A., Ohira, M., Schleiermacher, G., Schramm, A., Schulte, J.H., Wang, Q., Westermann, F., Speleman, F., Vandesompele, J., 2010. Accurate outcome prediction in neuroblastoma across independent data sets using a multigene signature. Clin. Cancer Res. 16, 1532–1541.

Fernandez, P., Solenthaler, M., Spertini, O., Quarroz, S., Rovo, A., Lovey, P.Y., Leoncini, L., Ruault-Jungblut, S., D'Asaro, M., Schaad, O., Docquier, M., Descombes, P., Matthes, T., Swiss Cytometry, S., 2012. Using digital RNA counting and flow cytometry to compare mRNA with protein expression in acute leukemias. PLoS One 7, e49010.

Furman, W.L., McGregor, L.M., McCarville, M.B., Onciu, M., Davidoff, A.M., Kovach, S., Hawkins, D., McPherson, V., Houghton, P.J., Billups, C.A., Wu, J., Stewart, C.F., Santana, V.M., 2012. A single-arm pilot phase II study of gefitinib and irinotecan in children with newly diagnosed high-risk neuroblastoma. Invest. New Drugs 30, 1660–1670.

Garcia, I., Mayol, G., Rios, J., Domenech, G., Cheung, N.K., Oberthuer, A., Fischer, M., Maris, J.M., Brodeur, G.M., Hero, B., Rodriguez, E., Sunol, M., Galvan, P., de Torres, C., Mora, J., Lavarino, C., 2012. A three-gene expression signature model for risk stratification of patients with neuroblastoma. Clin. Cancer Res. 18, 2012–2023.

Geiss, G.K., Bumgarner, R.E., Birditt, B., Dahl, T., Dowidar, N., Dunaway, D.L., Fell, H.P., Ferree, S., George, R.D., Grogan, T., James, J.J., Maysuria, M., Mitton, J.D., Oliveri, P., Osborn, J.L., Peng, T., Ratcliffe, A.L., Webster, P.J., Davidson, E.H., Hood, L., Dimitrov, K., 2008. Direct multiplexed measurement of gene expression with color-coded probe pairs. Nat. Biotechnol. 26, 317–325.

Kaplan, E.L., Meier, P., 1958. Nonparametric estimation from incomplete observations. J. Am. Stat. Assoc. 53, 457–481.

Kletzel, M., Katzenstein, H.M., Haut, P.R., Yu, A.L., Morgan, E., Reynolds, M., Geissler, G., Marymount, M.H., Liu, D., Kalapurakal, J.A., Shore, R.M., Bardo, D.M., Schmoldt, J., Rademaker, A.W., Cohn, S.L., 2002. Treatment of high-risk neuroblastoma with triple-tandem high-dose therapy and stem-cell rescue: results of the Chicago Pilot II study. J. Clin. Oncol. 20, 2284–2292.

Kreissman, S.G., Seeger, R.C., Matthay, K.K., London, W.B., Sposto, R., Grupp, S.A., Haas-Kogan, D.A., Laquaglia, M.P., Yu, A.L., Diller, L., Buxton, A., Park, J.R., Cohn, S.L., Maris, J.M., Reynolds, C.P., Villablanca, J.G., 2013. Purged versus non-purged peripheral blood stem-cell transplantation for high-risk neuroblastoma (COG A3973): a randomised phase 3 trial. Lancet Oncol. 14, 999–1008.

Kulkarni, M.M., 2011. Digital multiplexed gene expression analysis using the NanoString nCounter system. Curr. Protoc. Mol. Biol. 94, 25B.10.1–25B.10.17.

Malkov, V.A., Serikawa, K.A., Balantac, N., Watters, J., Geiss, G., Mashadi-Hossein, A., Fare, T., 2009. Multiplexed measurements of gene signatures in different analytes using the Nanostring nCounter assay system. BMC. Res. Notes 2, 80.

Maris, J.M., 2010. Recent advances in neuroblastoma. N. Engl. J. Med. 362, 2202–2211.

Maris, J.M., Hogarty, M.D., Bagatell, R., Cohn, S.L., 2007. Neuroblastoma. Lancet 369, 2106–2120.

Matthay, K.K., Reynolds, C.P., Seeger, R.C., Shimada, H., Adkins, E.S., Haas-Kogan, D., Gerbing, R.B., London, W.B., Villablanca, J.G., 2009. Long-term results for children with high-risk neuroblastoma treated on a randomized trial of myeloablative therapy followed by 13-cis-retinoic acid: a children's oncology group study. J. Clin. Oncol. 27, 1007–1013.

Northcott, P.A., Shih, D.J., Remke, M., Cho, Y.J., Kool, M., Hawkins, C., Eberhart, C.G., Dubuc, A., Guettouche, T., Cardentey, Y., Bouffet, E., Pomeroy, S.L., Marra, M., Malkin, D., Rutka, J.T., Korshunov, A., Pfister, S., Taylor, M.D., 2012. Rapid, reliable, and reproducible molecular sub-grouping of clinical medulloblastoma samples. Acta Neuropathol. 123, 615–626.

Oberthuer, A., Hero, B., Berthold, F., Juraeva, D., Faldum, A., Kahlert, Y., Asgharzadeh, S., Seeger, R., Scaruffi, P., Tonini, G.P., Janoueix-Lerosey, I., Delattre, O., Schleiermacher, G., Vandesompele, J., Vermeulen, J., Speleman, F., Noguera, R., Piqueras, M., Benard, J., Valent, A., Avigad, S., Yaniv, I., Weber, A., Christiansen, H., Grundy, R.G., Schardt, K., Schwab, M., Eils, R., Warnat, P., Kaderali, L., Simon, T., Decarolis, B., Theissen, J., Westermann, F., Brors, B., Fischer, M., 2010. Prognostic impact of gene expression-based classification for neuroblastoma. J. Clin. Oncol. 28, 3506–3515.

Payton, J.E., Grieselhuber, N.R., Chang, L.W., Murakami, M., Geiss, G.K., Link, D.C., Nagarajan, R., Watson, M.A., Ley, T.J., 2009. High throughput digital quantification of mRNA abundance in primary human acute myeloid leukemia samples. J. Clin. Invest. 119, 1714–1726.

Santana, V.M., Furman, W.L., Billups, C.A., Hoffer, F., Davidoff, A.M., Houghton, P.J., Stewart, C.F., 2005. Improved response in high-risk neuroblastoma with protracted topotecan administration using a pharmacokinetically guided dosing approach. J. Clin. Oncol. 23, 4039–4047.

Schramm, A., Schulte, J.H., Klein-Hitpass, L., Havers, W., Sieverts, H., Berwanger, B., Christiansen, H., Warnat, P., Brors, B., Eils, J., Eils, R., Eggert, A., 2005. Prediction of clinical outcome and biological characterization of neuroblastoma by expression profiling. Oncogene 24, 7902–7912.

Schulte, J.H., Schowe, B., Mestdagh, P., Kaderali, L., Kalaghatgi, P., Schlierf, S., Vermeulen, J., Brockmeyer, B., Pajtler, K., Thor, T., de Preter, K., Speleman, F., Morik, K., Eggert, A., Vandesompele, J., Schramm, A., 2010. Accurate prediction of neuroblastoma outcome based on miRNA expression profiles. Int. J. Cancer 127, 2374–2385.

Shimada, H., Ambros, I.M., Dehner, L.P., Hata, J., Joshi, V.V., Roald, B., Stram, D.O., Gerbing, R.B., Lukens, J.N., Matthay, K.K., Castleberry, R.P., 1999. The international neuroblastoma pathology classification (the Shimada system). Cancer 86, 364–372.

Storey, J.D., 2002. A direct approach to false discovery rates. J. Roy Stat. Soc. Ser. B 64, 479–498.

Stricker, T.P., Henriksen, K.J., Tonsgard, J.H., Montag, A.G., Krausz, T.N., Pytel, P., 2013. Expression profiling of 519 kinase genes in matched malignant peripheral nerve sheath tumor/plexiform neurofibroma samples is discriminatory and identifies mitotic regulators BUB1B, PBK and NEK2 as overexpressed with transformation. Mod. Pathol. 26, 930–943.

Vermeulen, J., De Preter, K., Naranjo, A., Vercruysse, L., Van Roy, N., Hellemans, J., Swerts, K., Bravo, S., Scaruffi, P., Tonini, G.P., De Bernardi, B., Noguera, R., Piqueras, M., Canete, A., Castel, V., Janoueix-Lerosey, I., Delattre, O., Schleiermacher, G., Michon, J., Combaret, V., Fischer, M., Oberthuer, A., Ambros, P.F., Beiske, K., Benard, J., Marques, B., Rubie, H., Kohler, J., Potschger, U., Ladenstein, R., Hogarty, M.D., McGrady, P., London, W.B., Laureys, G., Speleman, F., Vandesompele, J., 2009. Predicting outcomes for children with neuroblastoma using a multigene-expression signature: a retrospective SIOPEN/COG/GPOH study. Lancet Oncol. 10, 663–671.

Wagner, L.M., Billups, C.A., Furman, W.L., Rao, B.N., Santana, V.M., 2004. Combined use of erythropoietin and granulocyte colony-stimulating factor does not decrease blood transfusion requirements during induction therapy for high-risk neuroblastoma: a randomized controlled trial. J. Clin. Oncol. 22, 1886–1893.

Wang, Q., Diskin, S., Rappaport, E., Attiyeh, E., Mosse, Y., Shue, D., Seiser, E., Jagannathan, J., Shusterman, S., Bansal, M., Khazi, D., Winter, C., Okawa, E., Grant, G., Cnaan, A., Zhao, H., Cheung, N.K., Gerald, W., London, W., Matthay, K.K., Brodeur, G.M., Maris, J.M., 2006. Integrative genomics identifies distinct molecular classes of neuroblastoma and shows that multiple genes are targeted by regional alterations in DNA copy number. Cancer Res. 66, 6050–6062.

Wei, J.S., Greer, B.T., Westermann, F., Steinberg, S.M., Son, C.G., Chen, Q.R., Whiteford, C.C., Bilke, S., Krasnoselsky, A.L., Cenacchi, N., Catchpoole, D., Berthold, F., Schwab, M., Khan, J., 2004. Prediction of clinical outcome using gene expression profiling and artificial neural networks for patients with neuroblastoma. Cancer Res. 64, 6883–6891.